

Penultimate Unit Effects in Free Radical Copolymerization Studied Using the Individual Propagating Radical Concentrations from Electron Spin Resonance Spectroscopy

Per B. Zetterlund,* Shinji Tagashira, Kyoko Izumi, Yutaka Nagano, Makoto Azukizawa, Hirotomo Yamazoe, Masatsugu Kumagai, and Bunichiro Yamada*

Department of Applied Chemistry, Graduate School of Engineering, Osaka City University, Osaka 558-8585, Japan

Received May 6, 2002; Revised Manuscript Received July 31, 2002

ABSTRACT: The scope of the ESR technique has been expanded to enable direct measurement of the individual propagating radical concentrations in a binary free radical copolymerization. The ESR spectra observed during the copolymerization of the deuterated monomers styrene- d_5 and cyclohexyl methacrylate- d_5 in benzene at 60 °C could be accounted for as the superimposed spectra of the homopolymerization systems, the outermost regions of the spectrum unambiguously assigned to macroradicals with styrene- d_5 as the terminal unit. The penultimate model with an *implicit* penultimate unit effect (PUE) was fitted to the ratio of the propagating radical concentrations (A_{12}) and the copolymer composition, resulting in the radical reactivity ratios $s_1 = k_{211}/k_{111} = 0.45$ and $s_2 = k_{122}/k_{222} = 0.50$. Simultaneous fitting of A_{12} and the copolymerization propagation rate coefficient (\bar{k}_p) resulted in lower s values ($s_1 = 0.08$, $s_2 = 0.10$). Optimization procedures employing the penultimate model with an *explicit* PUE and the entire data set (copolymer composition, A_{12} and \bar{k}_p) indicated that the total sum of residuals could be further decreased compared with when the restriction of an *implicit* PUE was imposed on the model, but this was at the expense of the quality of the prediction of copolymer composition, which then became unacceptable.

Introduction

The copolymer composition equation based on the terminal model of free radical copolymerization was proposed in 1944^{1,2} and was followed by extensive research in the field almost exclusively focusing on copolymer composition while little attention was paid to the overall polymerization rate. The terminal model largely remained unchallenged until 1985, when Fukuda et al.^{3–8} showed that it fails to describe the overall copolymerization propagation rate coefficient (\bar{k}_p) although correctly describing the copolymer composition. A model which also takes into account the penultimate unit effect (PUE) of the propagating species, the penultimate model,^{2,9} has been found to be able to provide an accurate description of the PUE appearing in the value of \bar{k}_p while the copolymer composition remains unaffected. For the majority of copolymer systems studied following the work of Fukuda et al.^{3,4} in 1985, an implicit PUE appears to be operative; i.e., it can only be detected in the value of \bar{k}_p and not in the copolymer composition and the monomer sequence distribution.^{5,6,9–13} In other work where the implicit model was subjected to critical testing, it was found to fail in providing a complete description of the copolymerization kinetics.^{14–17}

Model compound studies have provided convincing support for γ -substituent effects on electron spin resonance (ESR) spectra and radical reactivity.^{18–22} Tanaka et al.²³ employed ESR spectroscopy and small model radicals to show that the substituents both at the penultimate and the penpenultimate position may affect

the spin distribution and conformation of the radical. Cywar and Tirrell²⁰ determined the relative rates of addition of 1-(1,3-diphenylpropyl) and 1-(3-cyano-1-phenylpropyl) radicals to styrene and acrylonitrile by end group analysis and detected a significant γ -substituent effect. Busfield et al.²¹ investigated the system AIBN/styrene/acrylonitrile using the nitroxide trapping technique and showed that the rate of addition of the second-generation cyanoisopropyl radical (from addition of a cyanoisopropyl radical to acrylonitrile) to styrene relative to acrylonitrile was significantly increased compared to that for the cyanoisopropyl radical.

Only a few examples of systems exhibiting an explicit PUE (which manifests itself in \bar{k}_p , the copolymer composition, and the monomer sequence distribution) have been reported.^{4,24,25} The origin of the PUE is still under debate; it has been proposed to be a result of polar effects,²² stabilization of the propagating radical by the penultimate unit,⁹ and entropic effects.²⁶ Investigations of the addition reactions of γ -substituted small radicals to alkenes by means of ab initio molecular orbital calculations have indicated that all three factors mentioned above are likely to contribute to the PUE in these reactions, suggesting that PUE's are *explicit* in nature.^{27–29}

ESR spectroscopy is a valuable experimental tool in the study of free radical polymerization processes.³⁰ It has been established that the technique yields reliable values of \bar{k}_p under appropriate experimental conditions.³¹ Sato et al. found that the ESR spectra of the copolymerization systems *N*-cyclohexyl maleimide/bis-(2-ethylhexyl) itaconate¹³ and *N*-cyclohexyl maleimide/di-*n*-butyl itaconate³² cannot be accounted for by simple addition of the homopolymerization spectra, thus indicating that some penultimate unit(s) (and possibly

* Corresponding authors. Telephone and fax: +81-6-6605-2797. E-mail: pbzetterlund@a-chem.eng.osaka-cu.ac.jp; yamada@a-chem.eng.osaka-cu.ac.jp.

penultimate unit(s)) influence the ESR splitting patterns. In their kinetic analyses, the value of \bar{k}_p as a function of monomer feed was estimated employing the total propagating radical concentration.^{10,12,13,32} The two individual radical concentrations as defined in the terminal model have to date not been directly measured for any copolymerization system. The ratio of the two radical concentrations (A_{12}) has however been estimated indirectly using ESR spin trapping experiments for the systems styrene/vinyl acetate^{33,34} and acrylonitrile/vinyl acetate.³⁵

The radical reactivity ratios ($s_1 = k_{211}/k_{111}$ and $s_2 = k_{122}/k_{222}$; see Appendix) for copolymerization systems have so far only been estimated by parameter optimization procedures involving copolymer composition and \bar{k}_p data (normally using sequential, not simultaneous,^{36,37} optimization procedures). Insensitivity of \bar{k}_p to the s -parameters results in great uncertainty in the values obtained.^{7,38–41} In the present study, we have for the first time succeeded in directly measuring the individual propagating radical concentrations in a binary copolymerization system by means of ESR spectroscopy using a system of deuterated monomers; 2,3,4,5,6-pentadeuteriostyrene (St- d_5) and cyclohexyl pentadeuteriomethacrylate (CHMA- d_5). This has made it possible to estimate s_1 and s_2 independently of \bar{k}_p data. This novel experimental quantity, in addition to the conventional data of copolymer composition and \bar{k}_p , should help us to achieve a better understanding of these systems, enable more rigorous testing of copolymerization models, and also make more accurate parameter optimizations possible. The results obtained are discussed within the framework of the penultimate models with an *implicit* or *explicit* PUE.

Experimental Section

St- d_5 was prepared as described in the literature,⁴² and CHMA- d_5 was prepared by esterification of pentadeuterio methacrylic acid.⁴³ Both monomers were purified by distillation under reduced pressure.

Polymerizations for conversion measurement by gravimetry were carried out in glass ampules sealed under vacuum (after at least three freeze–thaw cycles) at 60 °C with a total monomer concentration of 3.0 M in benzene initiated by 0.10 M dimethyl 2,2'-azobisisobutyrate (Wako Pure Chemicals, recrystallized from hexane). The polymer formed was isolated by pouring the contents of the ampule into a large amount of methanol and collecting the precipitate.

¹H NMR and ²H NMR spectra were recorded on a JEOL GX-400 spectrometer at 400 MHz in deuteriochloroform and chloroform, respectively, using tetramethylsilane as internal standard. The copolymer composition was determined by both ¹H NMR (from the ratio of the resonances corresponding to the methylene and methine protons of St- d_5 to that of the methine proton of the cyclohexyl ring of CHMA- d_5) and ²H NMR, using samples with conversion levels lower than 5%.

The propagation rate coefficients (\bar{k}_p as a function of monomer feed composition; throughout this paper, a bar over a parameter indicates its dependence on monomer feed composition) were determined by ESR quantification of the propagating radical concentrations at steady-state conditions of monomer conversion lower than a few percent. The rate of polymerization (R_p) was obtained by gravimetry at equally low conversion levels. When R_p is calculated from the gravimetric data, the differences in molecular weight of the monomers were corrected for by use of the copolymer composition curve. The values of \bar{k}_p were then obtained from the slope of plots of $\ln([M]_0/[M])$ vs t according to the integrated rate expression, (1), where $[M]$ and $[M^*]$ denote the total monomer and total propagating radical concentrations, respectively:

$$\ln \frac{[M]_0}{[M]_t} = \bar{k}_p [M^*] t \quad (1)$$

Molecular weights were measured with a Tosoh-800 series HPLC equipped with GPC columns using polystyrene standards.

ESR spectra were recorded on a Bruker ESP300 during polymerization in the cavity in a 5 mm o.d. quartz tube sealed under vacuum. 1,3,5-Triphenylverdazyl in benzene was used as a stable free radical for calibration of the relationship between ESR spectral signal intensity and the radical concentration. Great efforts were made to find the optimum conditions in terms of signal-to-noise ratio and resolution. Linearity between the double integral of the spectra of the polymerizations and the square root of the microwave power were confirmed to ensure that saturation did not occur. For each individual ESR measurement used in the quantification procedure, an additional measurement was carried out at higher microwave power to check for saturation.

Curve fitting procedures were performed employing *Mathematica*⁴⁴ version 4.0.2.0 (Wolfram Research, employed for all parameter optimizations involving \bar{k}_p and A_{12} data) and in-house software⁴⁵ (fitting of copolymer composition). The curve fittings carried out with *Mathematica* made use of a built-in tool that finds the minimum in a function ("FindMinimum"). A range of different starting values for the unknown parameters were used in all cases to ensure that global minima were found.

Results and Discussion

ESR Spectroscopy. In this study we set out to experimentally estimate the individual concentrations of the two propagating radical species M_1^* and M_2^* . In principle, this can be achieved if the ESR spectrum of the copolymerizing system can be accounted for as the sum of the spectra of the two homopolymerizing systems. The values of $[M_1^*]$ and $[M_2^*]$ can then be obtained by simulation even if the spectra corresponding to the two radicals overlap. If the spectra partially overlap, but the resolution is such that a certain peak or peaks in the integrated spectrum may be attributed to one of the radicals, the relative radical concentrations can be obtained straight from double integration of the ESR spectrum.

The copolymerization of two deuterated monomers was selected in the present study: St- d_5 (M_1) and CHMA- d_5 (M_2). The primary reason for choosing deuterated monomers was that the quantification of the two individual propagating radical concentrations relies on the penultimate unit having a negligible effect on the ESR spectra. The hyperfine coupling constant of deuterium is about 6.5 times smaller than that of a proton,⁴⁶ and consequently, any couplings of deuteriums on the penultimate monomer unit can be expected to have a small effect on the splitting pattern of the spectrum. Thus, by selection of a suitable pair of deuterated monomers, it was expected that the copolymerization spectra could be accounted for as the sum of the respective homopolymerization spectra. It is here important to stress that although the penultimate unit of a propagating species in general may influence the ESR splitting pattern,^{13,32} it cannot be concluded based on the absence of such an effect that there is no PUE on the polymerization kinetics.

The homopolymerization of St- d_5 ⁴² results in a significantly broadened four-line spectrum of intensity ratio 1:3:3:1 (Figure 1), because the hyperfine coupling constants of the protons of the aromatic ring are too small for observable splitting. The propagating species

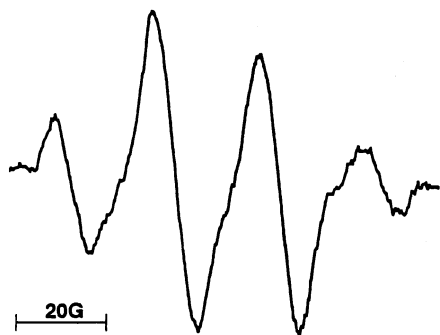


Figure 1. ESR spectrum recorded during the polymerization of 3.0 M St-*d*₅ in benzene initiated by 0.10 M dimethyl 2,2'-azobisisobutyrate at 60 °C.

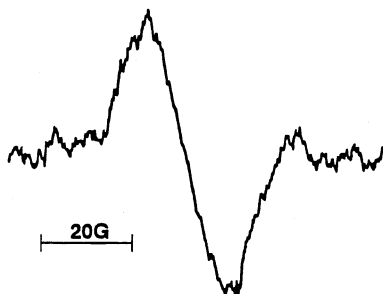


Figure 2. ESR spectrum recorded during the polymerization of 3.0 M CHMA-*d*₅ in benzene initiated by 0.10 M dimethyl 2,2'-azobisisobutyrate at 60 °C.

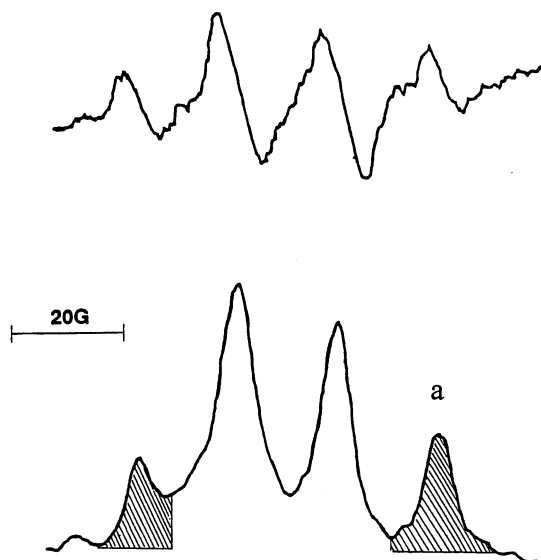


Figure 3. Differential and integrated ESR spectra recorded during the copolymerization of St-*d*₅ and CHMA-*d*₅ ($f_1 = 0.67$; [St-*d*₅] + [CHMA-*d*₅] = 3.0 M) in benzene initiated by 0.10 M dimethyl 2,2'-azobisisobutyrate at 60 °C. The shaded peaks in the integrated spectrum correspond to propagating radicals with St-*d*₅ as terminal unit.

in the homopolymerization of CHMA-*d*₅ gives rise to a broad singlet (Figure 2). Furthermore, CHMA-*d*₅ was chosen as a comonomer bearing in mind that the relatively low value of the termination rate coefficient during its homopolymerization yields a high steady-state free radical concentration suitable for ESR observation.⁴⁷ As expected, the spectra observed during the copolymerization of St-*d*₅/CHMA-*d*₅ could be accounted for as the sum of the spectra of the propagating species in the homopolymerizations of St-*d*₅ and CHMA-*d*₅, at all monomer feed compositions (Figure 3). This indicates

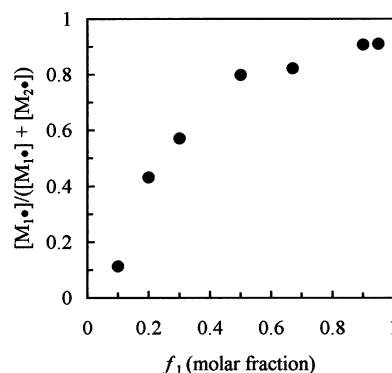


Figure 4. Fraction of propagating radicals with St-*d*₅ as terminal unit as a function of f_1 .

that the penultimate unit has a very small effect on the overall spectrum for this particular system. The coupling constants of the α - and β -protons of the St-*d*₅ terminated radicals are sufficiently large for part of the spectrum corresponding to these radicals to not overlap with CHMA-*d*₅ terminated radicals. The outermost peaks of the integrated ESR spectrum of the copolymerization system (shaded in Figure 3) could be unambiguously assigned to propagating species having the terminal unit St-*d*₅. The ratio of the concentrations of propagating species with St-*d*₅ and CHMA-*d*₅ as terminal units, $[M_1^{\bullet}]/[M_2^{\bullet}] = A_{12}$, could thus be obtained from the relative areas of the peaks. Peak "a" was clearly resolved from the rest of the spectrum, and the ratio (denoted X) of the area of this peak to the total area was employed for estimation of A_{12} according to the relationship $A_{12} = 8X/(1 - 8X)$.

Radical Concentrations. The individual propagating radical concentrations were estimated for a range of monomer feed compositions (f_1). If the terminal unit of each propagating radical changes a sufficient number of times during its lifetime, then the quantity A_{12} is governed solely by the relative rates of cross-propagation. The degrees of polymerization were high enough (>100) for this requirement to be fulfilled. Application of the stationary state approximation to each radical concentration leads to eq 2:

$$\bar{k}_{12}[M_1^{\bullet}][M_2] = \bar{k}_{21}[M_2^{\bullet}][M_1] \quad (2)$$

Rearrangement gives an expression for A_{12} :

$$A_{12} = \frac{[M_1^{\bullet}]}{[M_2^{\bullet}]} = \frac{\bar{k}_{21}}{\bar{k}_{12}} \frac{[M_1]}{[M_2]} \quad (3)$$

The fraction of propagating species having St-*d*₅ as terminal unit (M_1^{\bullet}) vs monomer feed composition is displayed in Figure 4. For the main part of the monomer feed range ($0.10 < f_1 < 0.90$), the fraction of M_1^{\bullet} radicals is greater than the fraction of M_1 in the monomer feed, indicating that a CHMA terminated radical reacts faster with St than a St-terminated radical with CHMA. According to the penultimate unit model for propagation, the value of \bar{k}_{12} is the sum of k_{112} and k_{212} weighted according to the relative proportions of the propagating species with penultimate unit M_1 and M_2 (eq 4):

$$\bar{k}_{12} = k_{112} \left(\frac{[M_1 M_1^{\bullet}]}{[M_1^{\bullet}]} \right) + k_{212} \left(\frac{[M_2 M_1^{\bullet}]}{[M_1^{\bullet}]} \right) \quad (4)$$

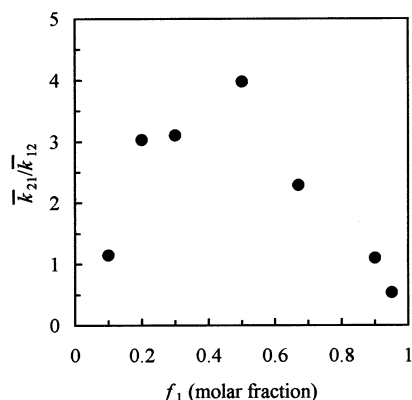


Figure 5. Ratio $\bar{k}_{21}/\bar{k}_{12}$ (from eq 3) plotted vs f_1 .

The expression for \bar{k}_{21} can be obtained by interchanging the subscripts 1 and 2 in eq 4. The ratio $\bar{k}_{21}/\bar{k}_{12}$, obtained from eq 3, is plotted vs monomer feed composition in Figure 5. For most of the monomer feed range, \bar{k}_{21} is greater than \bar{k}_{12} by roughly a factor of between 2 and 4. In the absence of a PUE and any solvent effects,⁴⁸ the ratio $\bar{k}_{21}/\bar{k}_{12}$ would be independent of the monomer feed composition. The terminal model predicts $\bar{k}_{21}/\bar{k}_{12} = 1.89$ based on the values of r_1 , r_2 , k_{111} and k_{222} reported later in this paper. Fukuda et al.⁴⁹ showed for the system St/MMA that there is no significant difference between \bar{k}_p as a function of monomer feed for bulk and a 50% solution in toluene, strongly suggesting the absence of any significant solvent effects. In view of these findings, it is considered highly improbable that any solvent/medium related effects constitute the origin of the monomer feed dependency of $\bar{k}_{21}/\bar{k}_{12}$ observed in the current system. The behavior of $\bar{k}_{21}/\bar{k}_{12}$ is ascribed to the dependences on the monomer feed of \bar{k}_{12} and \bar{k}_{21} , which in turn can be explained by the monomer feed dependences of the ratios $[M_1M_1^{\bullet}]/[M_1^{\bullet}]$ and $[M_2M_1^{\bullet}]/[M_1^{\bullet}]$ according to eq 4. The behavior of $\bar{k}_{21}/\bar{k}_{12}$ is consistent with a PUE on the cross-propagation step, and it cannot be concluded from this dependence on monomer feed composition whether there is a PUE on the homopropagation step (i.e., whether $k_{111} = k_{211}$ and $k_{222} = k_{122}$, or in other words whether $s_1 = s_2 = 1$). It is also not possible to discriminate between the *implicit* and *explicit* PUE based on these data only.

Copolymer Composition. The copolymer composition determined by ^1H NMR and ^2H NMR resulted in good agreement as shown in Figure 6. The copolymer composition (using the ^1H NMR data only) was fitted to the terminal model using a nonlinear least squares procedure,⁴⁵ resulting in $r_1 = 0.29$ and $r_2 = 0.49$. The copolymer composition can thus be adequately described by the terminal model; i.e., no PUE can be detected in the copolymer composition. However, it should here be recalled that a satisfactory fit of the terminal model to copolymer composition data does not constitute definitive evidence of the absence of *explicit* PUE's.^{3,50}

Estimation of s_1 and s_2 from A_{12} . The conventional way of estimating the radical reactivity ratios s_1 and s_2 is to fit the penultimate model, with the added restriction of the PUE being *implicit* in nature, to \bar{k}_p as a function of monomer feed composition using values of r_1 and r_2 from the copolymer composition. We here report the estimation of s_1 and s_2 by an alternative means, i.e., by use of the experimental quantity A_{12} as obtained by ESR. The value of A_{12} is related to s_1 and

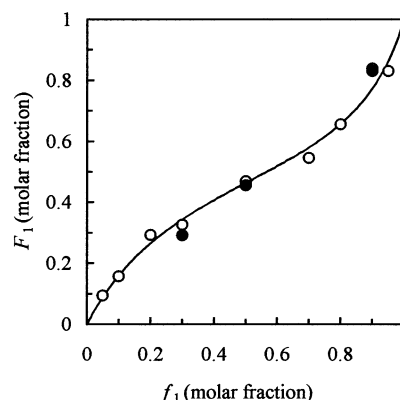


Figure 6. Copolymer composition estimated by ^1H NMR (\circ) and ^2H NMR (\bullet) for St- d_5 /CHMA- d_5 vs f_1 . The line is a best fit of the ^1H NMR data using the terminal model ($r_1 = 0.29$, $r_2 = 0.49$).

s_2 via eq 5, which is readily derived from eqs 2, 15, and 16 (see Appendix) (assuming an *implicit* PUE):

$$A_{12} = \frac{[M_1^{\bullet}]}{[M_2^{\bullet}]} = \frac{r_1 f_1 \bar{k}_{22}}{r_2 f_2 \bar{k}_{11}} = \frac{\left(r_1 f_1 + \frac{f_2}{s_1}\right)(r_2 f_2 + f_1) r_1 f_1 k_{222}}{\left(r_2 f_2 + \frac{f_1}{s_2}\right)(r_1 f_1 + f_2) r_2 f_2 k_{111}} \quad (5)$$

The homopropagation rate coefficients were determined by ESR quantification of the propagating radical concentrations combined with R_p measurements using gravimetry, resulting in k_{111} (St- d_5) = $325 \text{ M}^{-1} \text{ s}^{-1}$ and k_{222} (CHMA- d_5) = $1040 \text{ M}^{-1} \text{ s}^{-1}$. Only the propagation rate coefficients for the nondeuterated analogues have been determined by pulsed-laser polymerization (PLP): St (60 °C),⁵¹ $339 \text{ M}^{-1} \text{ s}^{-1}$; CHMA (60 °C),⁵² $1590 \text{ M}^{-1} \text{ s}^{-1}$ (calculated from the reported Arrhenius parameters). It has previously been shown that no major change in the value of k_p accompanies nuclear deuteration.^{53,54} Parameter optimization procedures were carried out to estimate the values of s_1 and s_2 from the A_{12} data, using r_1 and r_2 obtained from the copolymer composition. To obtain correct parameter estimates for s_1 and s_2 from the experimental quantity A_{12} , it is of primary importance to use appropriate weighting of the residuals. The error structure in the dependent variable (A_{12}) determines the choice of these weighting factors (the error in the independent variable (f_1) was assumed negligible in all optimizations). In the absence of replicas of each data point (required in order to have knowledge of the error structure), and although it is likely that the experimental error in A_{12} increases as the St- d_5 content is reduced (due to the decrease in signal-to-noise ratio with regards to the two outermost peaks), a constant relative error in the dependent variable was assumed rather than adopting some arbitrary error structure.

The conventional nonlinear least-squares method with constant relative error⁵⁵ results in a best fit where model estimates that are *lower* than the experimental data points are disproportionately favored, thus biasing the optimizations in an irrational manner (the effect is exaggerated when the dependent variable changes orders of magnitude). To circumvent this dilemma, it was decided to estimate s_1 and s_2 as the parameter

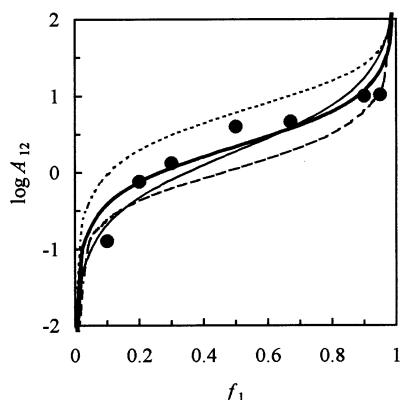


Figure 7. Model predictions of A_{12} (*implicit* PUE). Thick black line: best fit giving $s_1 = 0.45$ and $s_2 = 0.50$. Dotted line: $s_1 = 0.20$ and $s_2 = 0.70$. Dashed line: $s_1 = 0.60$ and $s_2 = 0.30$. Thin black line: terminal model ($s_1 = s_2 = 1$). (●) ESR.

values that satisfy the minimum of the sum of the residuals (SR) as in eq 6

$$SR(s_1, s_2) = \sum_i \left| \log \left(\frac{y_i}{g(x_i; s_1, s_2)} \right) \right| \quad (6)$$

where y_i is the dependent variable (A_{12} in this case) in the function $g(x_i; s_1, s_2)$, where x_i represents monomer feed (f_i) data. By using this alternative approach, which also gives the residuals equal weight, model predictions that deviate from the experimental data by a certain percentage will give the same SR regardless of whether the model over- or underestimates the experimental data. The optimizations converged on a global minimum (confirmed by manual inspection of the SR plane,⁵⁵ and by employing a range of different initial parameter values in the optimization procedures) at $s_1 = 0.45$ and $s_2 = 0.50$.

The model predictions and the ESR results are displayed in Figure 7. To illustrate the sensitivity of A_{12} on the parameters s_1 and s_2 , the model predictions for the ranges $0.20 \leq s_1 \leq 0.60$ and $0.30 \leq s_2 \leq 0.70$ are also displayed. All experimental data with the exception of the point at $f_1 = 0.10$ (which is expected to be the least reliable⁵⁶ in the data set because the value of the ratio X of the double integration of the ESR spectrum is the smallest here) are contained within the region defined by the two predictions corresponding to $s_1 = 0.20$ and $s_2 = 0.70$ (upper boundary) and $s_1 = 0.60$ and $s_2 = 0.30$ (lower boundary). All combinations of s values within $0.20 \leq s_1 \leq 0.60$ and $0.30 \leq s_2 \leq 0.70$ result in model predictions that lie between the two extremes, with the optimum condition located at $s_1 = 0.45$ and $s_2 = 0.50$. The terminal model prediction ($s_1 = s_2 = 1$) is also displayed in Figure 7. It appears as if the penultimate model with an *implicit* PUE, using r_1 and r_2 values estimated from the copolymer composition, can satisfactorily describe the ratio of the concentrations of the two types of propagating radical species for this particular system. The computation of a joint-confidence interval (JCI) for s_1 and s_2 according to the method of van Herk⁵⁵ is of limited meaning in this case since the SR of eq 6 refers to the logarithmic values of the data (thus yielding an extremely large JCI).

Estimation of s_1 and s_2 from A_{12} and \bar{k}_p . The estimation of s_1 and s_2 from \bar{k}_p data, using r_1 and r_2 from the copolymer composition data, is well-known to be fraught with difficulty.^{7,38–41} The JCI's are often very

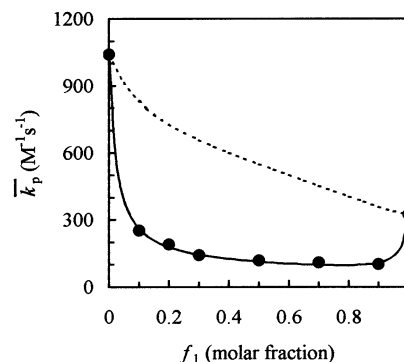


Figure 8. Penultimate model predictions of \bar{k}_p (*implicit* PUE). Full line: $s_1 = 0.08$ and $s_2 = 0.10$ from best fit of \bar{k}_p vs f_1 . Dotted line: $s_1 = 0.45$ and $s_2 = 0.50$ from best fit of A_{12} vs f_1 (*implicit* PUE). (●) Experimental.

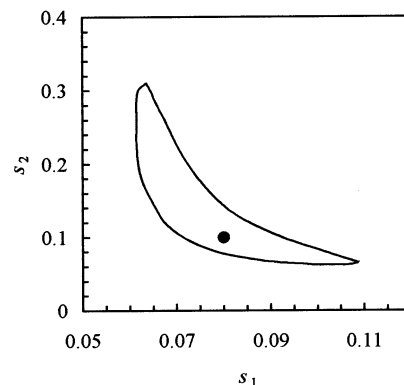


Figure 9. Joint-confidence interval at the 95% confidence level for s_1 and s_2 estimated from \bar{k}_p vs f_1 . Global minimum at $s_1 = 0.08$, $s_2 = 0.10$.

large, and in certain cases it is not possible to determine both s_1 and s_2 in this way. To be able to obtain consistent values from such optimization procedures, Fukuda et al.³⁹ proposed the use of the approximation $s = s_1 = s_2$, where s represents an “average PUE”. The value of \bar{k}_p as a function of f_1 is displayed in Figure 8. As is usually the case (but not always^{8,14}), the \bar{k}_p values are considerably lower than the arithmetic averages of the two homopolymerization k_p 's. The conventional approach to estimate the s values by nonlinear least-squares parameter optimization procedures of \bar{k}_p vs monomer feed composition data using r_1 and r_2 from the copolymer composition (i.e., assuming an *implicit* PUE) resulted in $s_1 = 0.08$ and $s_2 = 0.10$ and a close to perfect fit (Figure 8). Constant relative error in the dependent variable was assumed for the \bar{k}_p data. A JCI interval⁵⁵ at the 95% confidence level is displayed in Figure 9.

In view of the fact that it is difficult, and indeed sometimes impossible,^{7,38,39} to determine both s_1 and s_2 from \bar{k}_p data,^{7,38,39} simultaneous parameter optimization procedures using both data sets of A_{12} and \bar{k}_p appears promising with regards to the prospect of an improvement in the level of confidence in the s values. The penultimate model with an *implicit* PUE was thus fitted simultaneously to the A_{12} and \bar{k}_p data using eq 6. All data points were given equal weight, and constant relative error in the dependent variable was assumed for all data points. The optimum values obtained were $s_1 = 0.08$ and $s_2 = 0.10$. These values coincide with the result obtained using the \bar{k}_p data only, which may appear odd. However, this is merely a result of the fact that s values significantly higher than 0.10 result in considerable overestimation of \bar{k}_p , whereas the quality

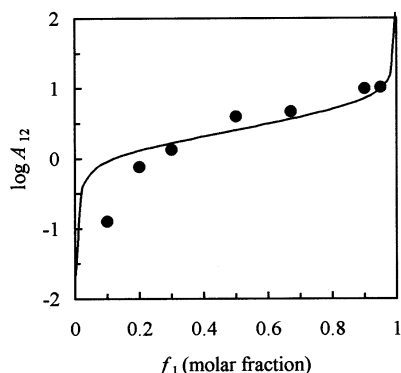


Figure 10. Penultimate model prediction (*implicit* PUE) of A_{12} for $s_1 = 0.08$ and $s_2 = 0.10$ from best fit of \bar{k}_p vs f_1 . (●) ESR.

of the A_{12} fit is less severely affected (in terms the SR according to eq 6) by a decrease in the s values from the optimum $s_1 = 0.45$ and $s_2 = 0.50$.

The model prediction of \bar{k}_p using $s_1 = 0.45$ and $s_2 = 0.50$ as obtained from the A_{12} fit results in significant overestimation as can be seen in Figure 8. Use of $s_1 = 0.08$ and $s_2 = 0.10$ from the \bar{k}_p fit and the simultaneous A_{12} and \bar{k}_p fit results in a relatively satisfactory model prediction of A_{12} over most of the monomer feed range (Figure 10), although at low St- d_5 content in the feed, A_{12} is considerably overestimated (by as much as a factor of approximately 10 at $f_1 = 0.10$). The relatively poor quality of the A_{12} prediction when using $s_1 = 0.08$ and $s_2 = 0.10$ (s values from the \bar{k}_p fit and the simultaneous A_{12} and \bar{k}_p fit), and the unsatisfactory prediction of \bar{k}_p using $s_1 = 0.45$ and $s_2 = 0.50$ (s values from the A_{12} fit) may be a result of: (i) experimental error in the A_{12} and/or \bar{k}_p data; (ii) error in the model input parameters r_1 , r_2 , k_{111} and k_{222} ; (iii) inadequacy of the model, or a combination of some or all of these factors.

Explicit PUE. Attempts were made to fit the penultimate model with an *explicit* PUE simultaneously to the copolymer composition, \bar{k}_p and A_{12} with the six unknown parameters r_{11} , r_{21} , r_{22} , r_{12} , s_1 , and s_2 . This was carried out using eq 6 for all three sets of experimental data (copolymer composition, \bar{k}_p and A_{12}), assuming constant relative error in the dependent variable for all data points. When performing optimizations of this sort where different data sets are employed simultaneously, it is not trivial how the residuals of the different sets should be weighted toward the total sum of residuals. In the absence of specific knowledge about the relative magnitude of the error in the three data sets, all data points were given equal weight. Parameter optimizations were performed for a range of different initial values of the unknown parameters. It was found that the optimization procedures did converge in all cases—however, the final parameter values obtained depended on the initial values used. In other words, it was not possible to confirm that the best solution in terms of a low value of the sum of the residuals as defined by eq 6 corresponded to the global minimum as opposed to a local minimum. It was possible to achieve a significantly lower total sum of residuals than for the *implicit* best fit. However, this was at the expense of the quality of the F_1 fit, which then became unacceptable. It can however not be excluded that a combination(s) of parameter values may exist that results in a better (*explicit*) model fit to \bar{k}_p and A_{12} while still achieving as

good a quality of the copolymer composition fit as when using the terminal model (i.e., *implicit* PUE).

Conclusions

The individual propagating radical concentrations in a binary copolymerization system have been directly measured for the first time by ESR spectroscopy by use of deuterated monomers: styrene- d_5 and cyclohexyl methacrylate- d_5 . The ESR spectra of the copolymerization system could be accounted for as the superimposed spectra of the homopolymerization systems, and the outermost regions of the spectrum for the copolymerization system could unambiguously be assigned to macroradicals with styrene- d_5 as the terminal unit.

The radical reactivity ratios (s_1 and s_2) were for the first time determined based on the penultimate model with an *implicit* PUE from the ratio of the concentrations of the two types of macroradicals (A_{12}) as a function of monomer feed without employing \bar{k}_p data. Extensive attempts to fit the entire data set (copolymer composition, A_{12} and \bar{k}_p) to the penultimate model with an *explicit* PUE (with six unknown parameters) appeared to indicate that no significant improvement in the overall predictive power of the model could be attained.

Appendix. Propagation Models

The terminal model. In the terminal model,^{1,2} it is assumed that only the terminal unit of the macroradical and the incoming monomer affect the propagation step. It consists of four propagation rate coefficients expressed in two monomer reactivity ratios:

$$r_i = \frac{k_{ii}}{k_{ij}} \quad i, j = 1, 2 \quad (i \neq j) \quad (7)$$

The overall propagation rate coefficient, \bar{k}_p , is defined by eq 8:

$$\frac{d([M_1] + [M_2])}{dt} = \bar{k}_p([M_1^\bullet] + [M_2^\bullet])([M_1] + [M_2]) \quad (8)$$

The individual rates of homopropagation and cross-propagation are related to the overall rate of copolymerization via eq 9:

$$\frac{d([M_1] + [M_2])}{dt} = k_{11}[M_1^\bullet][M_1] + k_{12}[M_1^\bullet][M_2] + k_{22}[M_2^\bullet][M_2] + k_{21}[M_2^\bullet][M_1] \quad (9)$$

The copolymer composition (F_i) is given by eq 10, and \bar{k}_p is related to the monomer reactivity ratios via eq 11:

$$F_i = \frac{f_i(r_i f_i + f_j)}{r_i f_i^2 + r_j f_j^2 + 2f_i f_j} \quad i, j = 1, 2 \quad (i \neq j) \quad (10)$$

$$\bar{k}_p = \frac{r_i f_i^2 + 2f_i f_j + r_j f_j^2}{\frac{r_i f_i}{k_{ii}} + \frac{r_j f_j}{k_{jj}}} \quad i, j = 1, 2 \quad (i \neq j) \quad (11)$$

The Penultimate Model. The penultimate model^{2,5} is based on the assumption that the nature of the penultimate unit also influences propagation, leading to eight propagation rate coefficients expressed in four monomer reactivity ratios (r_{ij} and r_{ji}) and two radical

reactivity ratios (s_j).

$$r_{ii} = \frac{k_{iii}}{k_{ijj}} \quad i, j = 1, 2 \ (i \neq j) \quad (12)$$

$$r_{ji} = \frac{k_{jii}}{k_{jjj}} \quad i, j = 1, 2 \ (i \neq j) \quad (13)$$

$$s_i = \frac{k_{jii}}{k_{iii}} \quad i, j = 1, 2 \ (i \neq j) \quad (14)$$

F_i and \bar{k}_p are expressed as in eqs 10 and 11, but here \bar{r}_i and \bar{k}_{ji} are functions of the monomer feed composition (f_j) according to eqs 15 and 16:

$$\bar{r}_i = \frac{r_{ji}(f_i r_{ii} + f_j)}{(f_i r_{ji} + f_j)} \quad i, j = 1, 2 \ (i \neq j) \quad (15)$$

$$\bar{k}_{ii} = \frac{k_{iii}(r_{ii} f_i + f_j)}{r_{ii} f_i + \frac{f_j}{s_i}} \quad i, j = 1, 2 \ (i \neq j) \quad (16)$$

The full penultimate model accounts for a so-called *explicit* PUE. A restricted version of the penultimate model describes a PUE that is *implicit* in nature, and was suggested by Fukuda et al.³ to account for the observation that the terminal model could describe copolymer composition but not \bar{k}_p for the system styrene/methyl methacrylate. If the PUE is *implicit*, there is no PUE on the monomer reactivity ratios

$$r_{ii} \left(= \frac{k_{iii}}{k_{ijj}} \right) = r_{ji} \left(= \frac{k_{jii}}{k_{jjj}} \right) = \frac{k_{ii}}{k_{jj}} = r_i \quad i, j = 1, 2 \ (i \neq j) \quad (17)$$

i.e., the penultimate unit affects reactivity but not selectivity. In other words, the PUE is independent of the type of the incoming monomer. It follows that an *implicit* PUE appears in \bar{k}_p but not copolymer composition or monomer sequence distribution data, and the monomer reactivity ratios are the same as those of the terminal model.

References and Notes

- (1) Mayo, F. R.; Lewis, F. M. *J. Am. Chem. Soc.* **1944**, *66*, 1594.
- (2) Merz, E.; T. Alfrey, J.; Goldfinger, G. J. *J. Polym. Sci.* **1946**, *1*, 75.
- (3) Fukuda, T.; Ma, Y.-D.; Inagaki, H. *Macromolecules* **1985**, *18*, 17.
- (4) Ma, Y.-D.; Fukuda, T.; Inagaki, H. *Macromolecules* **1985**, *18*, 26.
- (5) Fukuda, T.; Kubo, K.; Ma, Y.-D. *Prog. Polym. Sci.* **1992**, *17*, 875.
- (6) Fukuda, T.; Ide, N.; Ma, Y.-D. *Macromol. Symp.* **1996**, *111*, 305.
- (7) Coote, M. L.; Davis, T. P. *Prog. Polym. Sci.* **1999**, *24*, 1217.
- (8) Davis, T. P. *J. Polym. Sci., Part A: Polym. Chem.* **2001**, *39*, 597.
- (9) Fukuda, T.; Ma, Y.-D.; Inagaki, H. *Makromol. Chem. Rapid Commun.* **1987**, *8*, 495.
- (10) Sato, T.; Kitajima, T.; Seno, M.; Hayashi, Y. *J. Polym. Sci., Part A: Polym. Chem.* **1998**, *36*, 1449.
- (11) Ma, Y.-D.; Sung, K.-S.; Tsujii, Y.; Fukuda, T. *Macromolecules* **2001**, *34*, 4749.
- (12) Sato, T.; Shimooka, S.; Seno, M.; Tanaka, H. *Macromol. Chem. Phys.* **1994**, *195*, 833–843.
- (13) Sato, T.; Kawasaki, S.; Seno, M.; Tanaka, H. *Makromol. Chem.* **1993**, *194*, 2247.
- (14) Yee, L. H.; Heuts, J. P. A.; Davis, T. P. *Macromolecules* **2001**, *34*, 3581.
- (15) Coote, M. L.; Davis, T. P. *Macromolecules* **1999**, *32*, 3626.
- (16) Kukulj, D.; Davis, T. P. *Macromolecules* **1998**, *31*, 5668.
- (17) Morris, L. M.; Davis, T. P.; Chaplin, R. P. *Polymer* **2001**, *42*, 941.
- (18) Prementine, G. S.; Tirrell, D. A. *Macromolecules* **1987**, *20*, 3034.
- (19) Jones, S. A.; Prementine, G. S.; Tirrell, D. A. *J. Am. Chem. Soc.* **1985**, *107*, 5275.
- (20) Cywar, D. A.; Tirrell, D. A. *J. Am. Chem. Soc.* **1989**, *111*, 7544.
- (21) Busfield, W. K.; Jenkins, I. D.; Le., P. V. *J. Polym. Sci., Part A: Polym. Chem.* **1998**, *36*, 2169.
- (22) Giese, B.; Engelbrecht, R. *Polym. Bull. (Berlin)* **1984**, *12*, 55.
- (23) Tanaka, H.; Sasai, K.; Sato, T.; Ota, T. *Macromolecules* **1988**, *21*, 3534.
- (24) Hill, D. J. T.; O'Donnell, J. H.; O'Sullivan, P. W. *Macromolecules* **1982**, *15*, 960.
- (25) Hill, D. J. T.; Lang, A. P.; O'Donnell, J. H.; O'Sullivan, P. W. *Eur. Polym. J.* **1989**, *9*, 911.
- (26) Heuts, J. P. A.; Gilbert, R. G.; Maxwell, I. A. *Macromolecules* **1997**, *30*, 726.
- (27) Coote, M. L.; Davis, T. P.; Radom, L. *Macromolecules* **1999**, *32*, 2935.
- (28) Coote, M. L.; Davis, T. P.; Radom, L. *Macromolecules* **1999**, *32*, 5270.
- (29) Fischer, H.; Radom, L. *Angew. Chem., Int. Ed.* **2001**, *40*, 1340.
- (30) Yamada, B.; Westmoreland, D. G.; Kobatake, S.; Konosu, O. *Prog. Polym. Sci.* **1999**, *24*, 565.
- (31) Tonge, M. P.; Kajiwar, A.; Kamachi, M.; Gilbert, R. G. *Polymer* **1998**, *39*, 2305.
- (32) Sato, T.; Takahashi, K.; Tanaka, H.; Ota, T. *Macromolecules* **1991**, *24*, 2330.
- (33) O'Driscoll, K. F.; Tabner, B. J. *Eur. Polym. J.* **1992**, *28*, 333.
- (34) Lane, J.; Tabner, B. J. *Eur. Polym. J.* **1991**, *27*, 247.
- (35) Cheetham, P. F.; Tabner, B. J. *Eur. Polym. J.* **1993**, *29*, 451.
- (36) Hutchinson, R. A.; McMinn, J. H.; D. A. Paquet, J.; Beuermann, S.; Jackson, C. *Ind. Eng. Chem. Res.* **1997**, *36*, 1103.
- (37) Schweer, J. *Makromol. Chem., Theory Simul.* **1993**, *2*, 485.
- (38) Heuts, J. P. A.; Coote, M. L.; Davis, T. P.; Johnston, L. P. M. The Measurement and Meaning of Radical Reactivity Ratios. In *Controlled Radical Polymerization*; Matyjaszewski, K., Ed.; ACS Symposium Series 685; American Chemical Society: Washington, DC, 1998; Chapter 8.
- (39) Fukuda, T.; Ma, Y.-D.; Kubo, K.; Takada, A. *Polym. J. (Tokyo)* **1989**, *21*, 1003.
- (40) Coote, M. L.; Johnston, L. P. M.; Davis, T. P. *Macromolecules* **1997**, *30*, 8191.
- (41) Coote, M. L.; Zammit, M. D.; Davis, T. P.; Willett, G. D. *Macromolecules* **1997**, *30*, 8182.
- (42) Yamada, B.; Tagashira, S.; Sakamoto, K.; Nagano, Y.; Miura, Y. *Polym. Bull. (Berlin)* **1997**, *38*, 339.
- (43) Cox, R. F. B.; Scormont, R. J. *Organic Syntheses*; Wiley: New York, 1955; Collect. Vol. II, p 7.
- (44) Wolfram, S. *The Mathematica Book*, 4th ed.; Wolfram Media/Cambridge University Press: New York, 1999.
- (45) Yamada, B.; Itahashi, M.; Otsu, T. *J. Polym. Sci.: Polym. Chem. Ed.* **1978**, *16*, 1719.
- (46) Pilkington, S. A.; Pilkington, R. S.; Sutcliffe, L. H. *J. Chem. Soc., Faraday Trans.* **1983**, *79*, 925.
- (47) Matsumoto, A.; Mizuta, K.; Otsu, T. *J. Polym. Sci., Part A: Polym. Chem.* **1993**, *31*, 2531–2539.
- (48) Coote, M.; Davis, T. P.; Klumperman, B.; Monteiro, M. J. *J. Macromol. Sci.—Rev. Macromol. Chem. Phys.* **1998**, *C38*, 567–593.
- (49) Fukuda, T.; Kubo, K.; Mae, Y.-D.; Inagaki, H. *Polym. J.* **1987**, *19*, 523.
- (50) Moad, G.; Solomon, D. H.; Spurling, T. H.; Stone, R. A. *Macromolecules* **1989**, *22*, 1145.
- (51) Buback, M.; Gilbert, R. G.; Hutchinson, R. A.; Klumperman, B.; Kuchta, F.-D.; Manders, B. G.; O'Driscoll, K. F.; Russell, G. T. *Macromol. Chem. Phys.* **1995**, *196*, 3267.
- (52) Hutchinson, R. A.; Beuermann, S.; Paquet, D. A., Jr.; McMinn, J. H.; Jackson, C. *Macromolecules* **1998**, *31*, 1542.
- (53) Olaj, O. F.; Schnoll-Bitai, I. *Makromol. Chem., Rapid Commun.* **1990**, *11*, 459.
- (54) Pryor, W. A.; Henderson, R. W.; Patsiga, R. A.; Carroll, N. J. *Am. Chem. Soc.* **1966**, *88*, 1199.
- (55) van Herk, A. M. *J. Chem. Educ.* **1995**, *72*, 138.
- (56) Alfrey, T., Jr.; Bohrer, J. J.; Mark, H. *Copolymerization*; Interscience Publishers: New York, 1952.